Latin American Journal of Solids and Structures
www.lajss.org

Displacement ductility for seismic design of RC walls for low-rise housing

Abstract
The paper compares and discusses displacement ductility ratios of reinforced concrete walls typically used in one- and two-story houses. Ductility is investigated by assessing response measured on 39 walls tested under shaking table excitations and quasi-static lateral loads. Variables studied were the height-to-length ratio and walls with openings, type of concrete and, steel ratio and type of web reinforcement. An equation to estimate the available ductility of a wall is proposed. Based on statistical analysis of data, values of displacement ductility capacity are recommended. Displacement ductility ratios can be used to compute both strength modification and displacement amplification factors for code-based seismic design.

Keywords
Displacement, ductility, concrete wall, low-rise housing, seismic design.

Julian Carrillo *
Giovanni González
Astrid Rubiano

Department of Civil Engineering, Universidad Militar Nueva Granada, UMNG. Cr. 11 No. 101-80, Bogotá, Colombia.

*Author e-mail: wjcarrillo@gmail.com

1 INTRODUCTION

In low-rise reinforced concrete (RC) wall housing, 100-mm thick solid slabs or slabs made of precast elements are frequently used. Clear height of the walls is frequently 2400 mm, and house floor plan area varies between 35 and 65 m2. Foundations are strip footings made of RC beams that support a 100-mm thick floor slab. Because of the large wall-to-floor area ratio of these units, one- and two story high concrete wall structures are subjected to small demands of lateral displacements and seismic forces. This phenomenon has prompted housing designers to use concrete compressive strengths of 15 to 20 MPa, as well as 100-mm thick walls. Also, in zones where seismic demands are low, such that design controlled by vertical actions, the minimum web shear reinforcement prescribed by ACI 318-11 building code appears to be excessive for controlling diagonal tension cracking. As a result, web steel reinforcement ratios smaller than the minimum ratio prescribed by ACI 318-11 code and web shear reinforcement made of welded-wire mesh are frequently used. Nevertheless, due to the particularities of the RC walls in low-rise housing, most of the design recommendations are not directly applicable.

Two of the most important parameters for code-based seismic design of structures are the strength modification factors and displacement amplification factor. Strength modifications from the elastic strength demand are commonly accounted for using both reduction factor due to nonlinear hysteretic behavior and amplification factor due to overstrength. Displacement ductility ratio has been widely accepted as a useful performance indicator because of its apparent relationship with the strength reduction factor due to nonlinear hysteretic behavior. Low-rise shear walls reinforced conventionally with vertical and horizontal steel in the web have been shown to have ductility and energy dissipation capacities lower than RC structures that deform primarily in flexure (Hsu and Mansour, 2005).

The aim of this paper is to establish the maximum available displacement ductility for the seismic design of RC walls for low-rise housing. Values of the displacement ductility ratio have been proposed based on laboratory test results obtained from 39 concrete wall specimens tested under quasi-static reversed-cyclic lateral loads and shaking table excitations. Wall performance and failure modes are compared and discussed. Parameters for computing displacement ductility of low-rise RC walls, as the yield and maximum displacements, are discussed. The main parameters that affect the magnitude of the structural ductility ratio for these walls, as the height-to-length ratio and the type of web shear reinforcement, are also discussed. An equation to estimate the displacement ductility capacity of a particular wall is proposed. In addition, displacement ductility capacity for code-based seismic design is recommended.

2 DISPLACEMENT DUCTILITY

Design lateral strengths prescribed in earthquake-resistant design provisions are typically lower and in some cases much lower than the lateral strength required to maintain a structure in the elastic range in the event of severe earthquake ground motions. Strength modifications from the elastic strength demand are commonly accounted for using both reduction and amplification factors.

In earthquake-resistant design, the capability of a system or structural element to undergo large amplitude cyclic deformations, under a given ground motion, without excessive strength deterioration is typically given by the available ductility ratio, μ. Some loss of stiffness is inevitable, but excessive stiffness loss can lead to collapse (Park, 1988). Therefore, the structure should be able to sustain several cycles of inelastic deformation without significant loss of strength. Ductile structures are generally able to dissipate significant amounts of energy during those cyclic deformations. The more energy dissipated per cycle without excessive deterioration, the better the behavior of the structure (FEMA-451, 2006). These two attributes (inelastic deformation and energy dissipation) are essential in earthquake-resistant structures, since they must survive high deformations with no loss of strength and dissipate the high input of energy (Salse and Fintel, 1973).

Ductility ratios have been commonly expressed in terms of various response parameters related to deformations, namely displacements, rotations and curvatures. The displacement ductility ratio in cyclic loading is based on the envelope curve of the hysteretic loops that show the relation between the strength and displacement of a system or structural element. A typical envelope of the structural response is shown in Fig. 1. Idealizing the actual structural response curve by the linearly elastic-perfectly plastic curve, the displacement ductility ratio is defined as the ratio of maximum displacement (Δ_u) to the corresponding displacement at the onset of yielding (Δ_y), as follows (Miranda and Bertero, 1994):

$$\mu = \frac{\Delta_u}{\Delta_y} \tag{1}$$

The envelope of actual structural response shown in Figure 1 is representative of systems that can dissipate energy in a stable manner; i.e. structures controlled by flexural deformations. For other systems that involve severe strength and stiffness deterioration, the definition of yield displacement and maximum displacement in Eqn. 1 may be incorrect (Uang, 1989). There has been difficulty in reaching consensus within the research community as to the appropriate definition of yield and maximum displacements. The definitions of the yield and maximum displacement are not standardized and different definitions have been used in the past. Some of these approaches are discussed below.

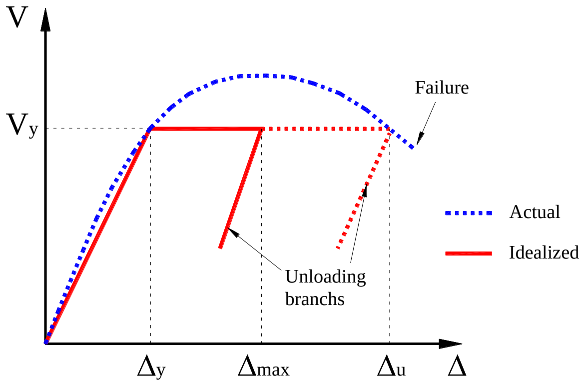

Figure 1: Envelope of actual and idealized structural response.

2.1 Yield displacement

When calculating ductility ratios, the definition of the yield deformation (displacement, rotation and curvature) often causes difficulty since the strength-deformation relation may not have a well-defined yield point. Various alternative definitions have been used by investigators to estimate the yield displacement, for instance, it has been defined as the intersection of the initial tangent stiffness with the nominal strength, the intersection of the secant stiffness through first yield with nominal strength, and the displacement at first yield (Priestley, 2000). According to Park (1988), the most realistic definition for reinforced concrete structures is the yield displacement of the equivalent elastic-perfectly plastic system with reduced stiffness found as secant stiffness at 75% of the peak lateral load of the actual system. For squat reinforced concrete walls, the displacement corresponding to the development of 75% or 80% of the maximum strength usually, though not necessarily, is close to the point of first significant yield (Salonikios et al., 2000). This definition takes the secant stiffness in order to include the reduction in stiffness due to cracking near the end of the elastic range.

2.2 Maximum displacement

The ductility required of a structure responding to a major earthquake (ductility demand) can be estimated by nonlinear time-history dynamic analysis. Ductility demand is computed using the same Eqn. 1, but using $\Delta_{\max}$ instead Δ_u (Fig. 1). The ductility required of the structure during response to a major earthquake needs to be matched by the available ductility of the structure (see Eqn. 1). To enable designers to ensure that structures have adequate available ductility to match the required ductility, procedures for evaluating the available ductility of structural members and their connections should be clearly defined (Park, 1988).

Displacement ductility capacity of concrete and masonry structures depends on a wide range of factors, including axial load ratio, reinforcement ratio, and structural geometry. The maximum displacement capacity has also been estimated using various assumptions by investigators, including displacement at peak strength, displacement corresponding to 20% up to 50% degradation from peak strength, and displacement at initial fracture of transverse reinforcement. Considering such a wide choice of limit displacements, there has been significant variation in the assessed displacement ductility capacity of structures (Priestley, 2000). When evaluating the most appropriate definition, it should be recognized that most structures have some capacity for deformation beyond the peak of the strength-deformation relation with some reduction in strength. It should be reasonable to recognize at least part of this post-peak deformation capacity. Therefore, a rational definition is the post-peak displacement when the load carrying capacity has undergone a small reduction, i.e. 20% or 25% (Park, 1988).

3 DUCTILITY RATIO FOR CODE-BASED SEISMIC DESIGN

Fig. 2a shows the required elastic strength expressed in terms of the maximum base shear that develops in the structure if it were to remain in the elastic range, V_e. The art of seismic-resistant design is in details; with good detailing, structures can be designed for force levels significantly lower than those required for elastic response (FEMA-451, 2006). Since a properly designed structure usually can provide a certain amount of ductility, the structure has capacity to dissipate hysteretic energy. Because of this energy dissipation, the structure can be designed economically and thus, the elastic design force V_e can be reduced to a yield strength level V_y, by the reduction factor due to nonlinear hysteretic behavior, R_μ (Fig. 2a) (Moroni et al., 1996); the corresponding maximum deformation demand is $\Delta_{\max}$.

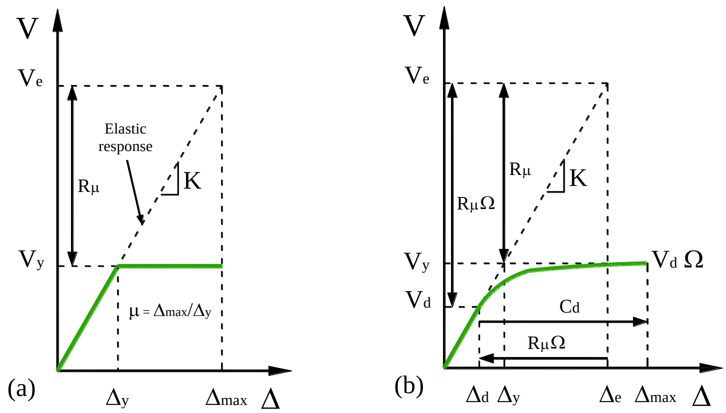

Figure 2: Idealized structural response: (a) equal displacement approximation, (b) design methodology in most building codes.

Since the calculation of V_y and $\Delta_{\max}$ involves nonlinear analysis, these quantities are generally not quantified in an explicit manner using code-based seismic design. Therefore, factor R_μ is defined as the ratio of the elastic to the inelastic strength demand (Miranda and Bertero, 1994), as follows:

$$R_\mu = \frac{V_e}{V_y} = \frac{F_y(\mu = 1)}{F_y(\mu = \mu_i)} \tag{2}$$

where $F_y(\mu = 1)$ is the lateral yield strength required to maintain the system elastic, and $F_y(\mu{=}\mu_i)$ is the lateral yield strength required to maintain the displacement ductility ratio demand μ, less than or equal to a predetermined maximum tolerable displacement (target) ductility ratio μ_i, when subjected to the same ground motion.

Parameter μ has been widely accepted as a useful performance indicator because of its apparent relationship to the strength reduction factor R_μ. As it is shown in Fig. 2a, the equal displacement approximation of seismic response implies that (Priestley, 2000):

$$\mu = R_\mu \tag{3}$$

It has been verified that the equal displacement approximation is non-conservative for short period structures, which roughly corresponds to the first region of the spectrum. Considering that the short period systems tend to display significant residual deformations, the equal energy approximation should be applied for these structures. This reduction is lower and depends on both the period of vibration T and the displacement ductility capacity μ. The strength reduction factor $\underline{R_\mu}$ can be calculated from the ductility ratio according to the period, as suggested by Newmark and Hall in ATC-19.

$$\begin{aligned} R_\mu &= 1.0 && \rightarrow \quad T < 0.03 s \\ R_\mu &= \sqrt{2\mu - 1} && \rightarrow \quad 0.12\ s \leq T \leq 0.5\ s \\ R_\mu &= \mu && \rightarrow \quad T \geq 1.0\ s \end{aligned} \tag{4}$$

The strength reserve that exists between the actual structural yield level V_y, and the code-prescribed first significant yield V_d, is defined in terms of the overstrength factor Ω (Fig. 2b). To estimate maximum expected displacements of the structure including effects of inelastic deformations, displacements from elastic analysis with reduced forces are amplified by the displacement amplification factor C_d. Factor C_d is defined as the ratio between the maximum expected nonlinear displacement during an earthquake Δ_{max}, and the elastic displacement induced by the reduced seismic forces Δ_d. Factor C_d can also be derived from Fig. 2b as follows (Uang, 1989).

$$C_d = \frac{\Delta_{max}}{\Delta_d} = \frac{\Delta_{max}}{\Delta_y} \frac{\Delta_y}{\Delta_d} = \mu\ \Omega \tag{5}$$

From these derivations, it is observed that C_d factor is function of structural overstrength factor and displacement ductility ratio.

4 EXPERIMENTAL PROGRAM

To assess experimentally the available ductility of concrete walls for low-rise housing during seismic loading, an extensive experimental program that comprised testing of 39 isolated cantilever walls was carried out at UNAM (Carrillo and Alcocer, 2012a, 2012b). Wall properties were those obtained from current design and construction practice found in typical low-rise housing in several Latin American countries.

4.1 Variables

The experimental program included the following variables: height-to-length ratio and walls with openings, concrete type, web steel ratio and type of web reinforcement.

Height-to-length ratio

Walls with height-to-length ratio (h_w/l_w) equal to 0.5, 1.0 and 2.0, and walls with door and window openings were tested. For walls tested in cantilever, the value of h_w/l_w is roughly equal to the value of the ratio between the bending moment and shear force times wall length (M/Vl_w). Full-scale wall thickness, tw, and clear height, h_w, were 100 mm and 2.4 m, respectively. Then, to achieve the h_w/l_w, length of walls was varied. Typical geometry and reinforcement layout of a wall specimen are shown in Fig. 3.

Thickness of boundary elements of walls was equal to web thickness. To better understand the strength mechanism that take place during shear failures observed in RC walls for low-rise housing, longitudinal boundary reinforcement was purposely designed to prevent flexural failure prior to achieving a shear failure.

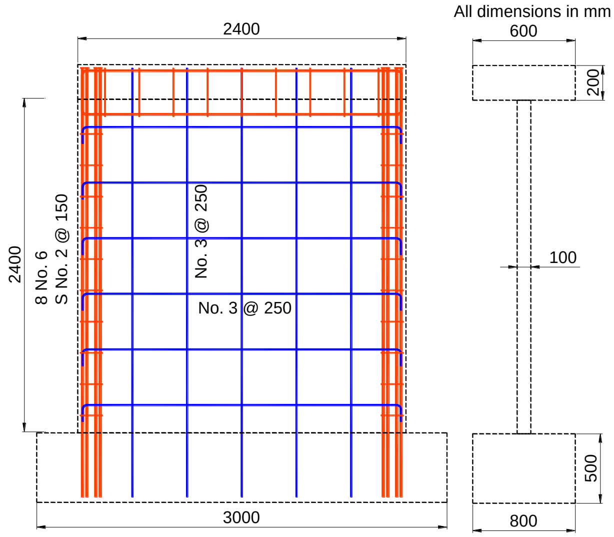

Figure 3: Geometry and reinforcement layout of a wall specimen: h_w/l_w=1.0, 100% of ρ_{min} and using deformed bars.

Concrete type

Normalweight (N), lightweight (L) and self-consolidating (S) concrete were included in the test series. Ready-mixed concrete was used for wall casting. Nominal concrete compressive strength, f_c', was 15 MPa for all types of concrete. Ranges of measured mechanical properties of concrete for the 39 specimens are presented in Table 1. Compressive strength (f_c), elastic modulus (E_c), tensile splitting strength (f_t), flexural strength (f_r) and specific dry weight (γ) are included in the table.

Table 1: Measured mechanical properties of concrete.

Property	Normalweight, N	Lightweight, L	Self-consolidating, S
f_c, MPa	16.0 – 24.7	10.8 – 26.0	22.0 – 27.1
E_c, MPa	8430 – 14750	6700 – 10790	8900 – 11780
f_t, MPa	1.55 – 2.20	1.14 – 1.76	1.58 – 1.98
fr, MPa	2.32 – 3.75	1.43 – 3.29	2.27 – 2.48
γ, kN/m^3	18.8 – 20.3	15.2 – 18.3	18.9

Web steel ratio

Three web steel ratios were studied; 100% of ρ_{min} (0.25%), 50% of ρ_{min} (0.125%), and 0% of ρ_{min} = without reinforcement (for reference only) were used. Minimum web steel ratio (ρ_{min}) was that prescribed by ACI 318-11. Tests of walls with 50% of ρmin were aimed at examining the performance of walls with a steel reinforcement smaller than the minimum prescribed by the code. Web reinforcement was placed in a single layer at wall mid-thickness and same ratios of horizontal and vertical reinforcement ($\rho_h = \rho_v$) were used.

Type of web reinforcement

Deformed bars (D) and welded-wire mesh made of small-gage wires (W) were used. Nominal yield strength of bars and wire reinforcement, f_y, was 412 MPa (for mild steel) and 491 MPa (for cold-drawn wires). Ranges of measured mechanical properties of steel reinforcement for the 39 specimens are presented in Table 2. Yield strength (f_y), ultimate strength (f_{su}) and elongation (EL) are included in the table.

Table 2: Measured mechanical properties of steel reinforcement.

Location	Boundary: deformed bar	Web: deformed bar, D	Web: welded-wire, W
Type	Mild	Mild	Cold-drawn
f_y , MPa	411 – 456	435 – 447	605 – 630
f_{su} , MPa	656 – 721	659 – 672	687 – 700
Elongation, %	9.1 – 16.0	10.1 – 11.0	1.4 – 1.9

In the cold-drawn wire reinforcement used in this study, the loading branch between onset of yielding and maximum deformation capacity (at fracture) was much shorter than that of mild-steel reinforcement. The behavior of wire reinforcement was characterized by fracture of material with a slight increment of strain (see the Elongation row in Table 2). In this study, the elongation capacity of wires was a key parameter for displacement capacity of walls reinforced in the web using this type of reinforcement.

Type of testing

Quasi-static (monotonic and reversed-cyclic) and dynamic (shaking table) testing series were included. In quasi-static testing, loading protocol consisted of a series of increasing amplitude cycles. For each increment, two cycles at same amplitude were applied (Sánchez, 2010). During shaking table tests, lightly-reduced scaled models were subjected to a series of base excitations represented by earthquake records associated to three limit states. An axial compressive stress of 0.25 MPa was applied on top of the walls and was kept constant during testing. This value corresponded to an average axial stress in the first floor walls of a two-story prototype house. Main characteristics of the 39 wall specimens are presented in Table 3.

5 TEST RESULTS AND DISCUSSION

Three failure modes were defined for assessing the observed wall behavior: a) when yielding of more than 70% of the web shear reinforcement and no web crushing of concrete was observed, a diagonal tension failure (DT) was defined; b) when yielding of some steel bars or wires and noticeable web crushing and spalling of concrete was observed, a diagonal compression failure (DC) was defined, and, c) when yielding of more than 70% of the web steel reinforcement and noticeable web crushing of concrete was observed, a mixed failure mode (DT-DC) was defined. Test results indicated that the contribution of wall sliding to the whole deformation was negligible for all tests (Carrillo and Alcocer, 2012a). Therefore, wall sliding at the base (SL) was not purposely included.

Failure modes of the 39 wall specimens are presented in Table 3. Walls reinforced with 50% of the minimum code-prescribed web steel reinforcement ratio and using deformed bars or welded-wire mesh, exhibited DT failure. Failure mode was governed by web inclined cracking of concrete at approximately 45° and yielding of most of web shear reinforcement prior to severe strength and stiffness decay. In walls reinforced with welded-wire mesh, fracture of wires after plastic yielding of web shear reinforcement was observed. Failure was brittle because of the limited elongation capacity of the wire mesh itself (see Table 2). In contrast, walls reinforced using deformed bars and minimum web steel ratio exhibited DT-DC failure. Typical final crack patterns of walls during shaking table tests are shown in Fig. 4.

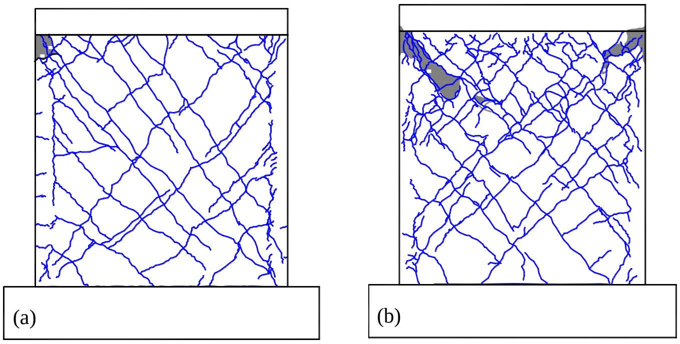

Figure 4: final crack patterns: (a) wall with $h_w/l_w = 1.0$, 50% of ρ_{min} and using welded-wire mesh (DT failure), (b) wall with $h_w/l_w = 1.0$, 100% of ρ_{min} and using deformed bars (DT-DC failure).

A previous study (Carrillo and Alcocer, 2012a) has determined the effect of each mode of deformation on the total displacement of wall specimens tested under shake table excitations. Results of that study demonstrated that the participation of shear displacements in the total story displacements was considerable because the behavior of specimens was always controlled by web shear deformations.

5.1 Ductility capacity of walls

The displacement ductility ratios were estimated using Eqn. 1 but expressing the maximum displacement and the conventional yield displacement in terms of drift ratios (R_u and R_y, respectively). In the case of an ideal elastic-perfectly plastic behavior, R_u and R_y are easily defined. However, for reinforced concrete elements, such as the low-rise walls considered in this study, it is not the case. Based on recommendations discussed in section 2.2, in this study the maximum drift ratio for evaluating ductility capacity, R_u, is associated with one of the two following scenarios: when 20% drop in peak shear strength (drift ratio that corresponds to 80% of the shear strength capacity in the post-peak descending branch of the envelope curve) is observed or when web shear reinforcement is fractured. In the specimens studied, the first scenario occurred in walls reinforced with deformed bars and the second scenario was observed in solid walls (no openings) with web shear reinforcement made of welded-wire mesh.

Table 3: Main characteristics and measured displacement of wall specimens.

Web reinforcement	Type of testing *	Wall	Type of concrete	h_w / l_w	$\rho_h = \rho_v$, %	Failure mode	R_y %	R_u % (+)	R_u % (-)	R_u % Mean	$\mu = R_u$ / R_y
No reinf.	SM	MCN0M	N	1.00	0	DT	0.31	0.60	-	0.60	1.91 $^{+}$
	SM	MCL0M	L	1.01	0	DT	0.30	0.63	-	0.63	2.09 $^{+}$
	SM	MCS0M	S	1.01	0	DT	0.49	0.88	-	0.88	1.80 $^{+}$
Welded-wire mesh, W	SC	MRN50mC	N	0.44	0.12	DT	0.12	0.50	0.40	0.45	3.62
	SC	MRNB50mC	N	0.44	0.13	DT	0.18	0.58	0.75	0.67	3.71
	SC	MRL50mC	L	0.45	0.12	DT	0.28	0.48	0.41	0.45	1.59
	SC	MCN50mC	N	1.00	0.12	DT	0.25	0.46	0.58	0.52	2.08
	SC	MCNB50mC	N	1.00	0.12	DT	0.17	0.34	0.46	0.40	2.42
	DY	MCN50mD	N	1.00	0.11	DT	0.28	0.51	0.58	0.54	1.93
	SC	MCL50mC	L	1.01	0.12	DT	0.42	0.66	0.60	0.63	1.51
	DY	MCL50mD	L	1.00	0.11	DT	0.42	0.69	0.61	0.65	1.55
	SC	MEN50mC	N	1.94	0.12	DT	0.35	0.75	0.61	0.68	1.91
	SC	MEL50mC	L	1.99	0.12	DT	0.38	0.80	0.61	0.71	1.87
	SC	MVN50mC	N	§	0.11	DT	0.27	0.40	0.41	0.40	1.48
	DY	MVN50mD	N	§	0.11	DT	0.25	0.51	0.38	0.44	1.78
Deformed bars, D	SC	MRN50C	N	0.45	0.14	DT	0.45	1.01	1.00	1.01	2.25
	SC	MRN100C	N	0.45	0.28	DC-SL	0.43	0.78	0.81	0.79	1.85 $^{+}$
	SC	MRL100C	L	0.45	0.28	SL	0.40	1.21	1.19	1.20	3.01 $^{+}$
	SM	MCN50M	N	1.01	0.14	DT	0.57	1.98	-	1.98	3.46 $^{+}$
	SC	MCN50C	N	1.01	0.14	DT	0.27	1.00	1.04	1.02	3.77
	SC	MCN50C-2	N	1.00	0.14	DT	0.20	0.49	0.95	0.72	3.64
	SM	MCL50M	L	1.01	0.14	DT	0.46	1.20	-	1.20	2.60 $^{+}$
	SC	MCL50C @	L	1.01	0.14	DT	0.35	0.70	0.68	0.69	1.97 $^{+}$
	SC	MCL50C-2	L	0.99	0.14	DT	0.30	1.21	1.15	1.18	3.92
	SC	MCS50C @	S	1.01	0.14	DT	0.50	0.97	1.09	1.03	2.08 $^{+}$
	SC	MCS50C-2	S	1.00	0.14	DT	0.20	0.46	0.73	0.59	2.96
	SM	MCN100M	N	1.01	0.28	DC-DT	0.45	1.71	-	1.71	3.77 $^{+}$
	SC	MCN100C	N	1.01	0.28	DC-DT	0.32	1.51	1.18	1.34	4.19
	DY	MCN100D	N	1.00	0.26	DT-DC	0.32	0.60	0.55	0.58	1.81
	SM	MCL100M	L	1.01	0.28	DC-DT	0.47	1.67	-	1.67	3.54 $^{+}$
	SC	MCL100C	L	1.01	0.28	DC	0.39	1.00	0.98	0.99	2.55
	SC	MCL100C-2	L	1.01	0.29	DC	0.45	1.60	1.41	1.51	3.33
	DY	MCL100D	L	1.00	0.27	DT-DC	0.37	0.62	0.84	0.73	1.99
	SM	MCS100M	S	1.01	0.28	DT-DC	0.63	2.25	-	2.25	3.57 $^{+}$
	SC	MCS100C	S	1.01	0.28	DT-DC	0.66	1.37	1.61	1.49	2.27
	SC	MEN50C	N	1.95	0.14	DT	0.67	2.15	1.99	2.07	3.08
	SC	MEN100C	N	1.96	0.28	DC-DT	0.79	1.79	1.81	1.80	2.27
	SC	MVN100C	N	§	0.26	DT-DC	0.37	0.78	1.41	1.09	2.94
	DY	MVN100D	N	§	0.26	DT-DC	0.36	0.88	0.77	0.82	2.29
Walls with web shear reinforcement made of welded wire mesh								Mean			2.12
								Coefficient of variation, CV (%)			34.9
Walls with web shear reinforcement made of deformed bars								Mean			2.88
								Coefficient of variation, CV (%)			25.3

* SM and SC = quasi-static (monotonic and reversed-cyclic), DY = dynamic (shaking table), § Wall with openings, @ Maximum displacement capacity was not attained, $^{+}$ Data not included to compute the mean of μ.

As discussed earlier, the response of reinforced concrete walls controlled by shear deformations is different to that of the elastic-perfectly plastic system and thus, ductility should be cautiously assessed because most of the times the yield displacement is not well-defined. Similarly to studies of low-rise concrete walls (Hsu, 2005; Salonikios et al., 2000), in this study, yield drift ratio, R_y, is associated to the development of 80% of the maximum strength.

For walls tested, drift ratios R_u and R_y were determined from hysteresis curves measured during shaking table and quasi-static tests of RC walls. Measured drift ratios R_u and R_y are included in Table 3. Values of R_u are the average for the two directions of in-plane displacement (i.e. push and pull directions). The values given in Table 3 indicate that positive and negative R_u values of a given wall were comparable. Therefore, the mean value of the positive and negative R_u values is used to compute the ductility capacity of walls, μ.

Measured data of displacement ductility capacity as a function of the M/Vl_w ratio are shown in Fig. 5. To reflect the behavior of walls under cyclic loading only, experimental data was taken from the series of shake table and quasi-static reversed-cyclic tests. Walls with openings were not included as they are not associated with a unique M/Vl_w ratio. Two of the walls tested are not included in the table because their displacement capacity was not attained; they were rehabilitated and retested (Table 3).

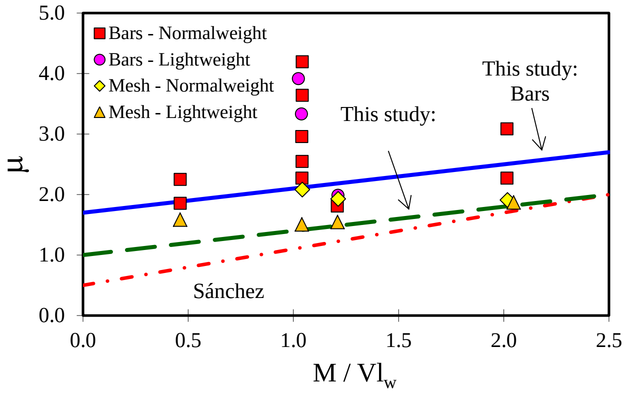

Figure 5: Relationship between μ and M/Vl_w ratio.

Results of equation proposed by Sánchez (2010) are included in the Fig. 5. When comparing measured data with Sánchez's equation, it is concluded that Sánchez's model underestimated the displacement ductility capacity of walls reinforced with deformed bars. Following trends from experimental results, it is proposed to estimate the displacement ductility capacity of a particular wall using Eqn. 6. Results of the proposed equation are shown in Fig. 5.

$$\mu = \mu_0 + 0.4\left(\frac{M}{V\,l_w}\right) \tag{6}$$

Values of μ_0 were derived from linear regression analysis. For walls with web shear reinforcement made of deformed bars and welded-wire mesh, μ_0 is equal to 1.7 and 1.0, respectively. Values of μ_0 were selected to provide a conservative prediction; for instance, the measured ductility capacity of most of the walls is higher than that predicted using the proposed equation. It is observed that a well-defined trend between displacement ductility capacity and M/Vl_w is lacking, mainly for squat walls ($M/Vl_w \approx 1.0$). It is also observed comparable behaviors between walls made of normalweight and lightweight concretes. Main reason of the scatter of data is the definition of R_y for low-rise concrete walls whose behavior is significantly different to that of the elastic-perfectly plastic.

5.2 Ductility capacity for code-based design

Analyzing trends of displacement ductility capacity, μ (Fig. 5), it is evident that the type of web shear reinforcement and the h_w/l_w ratio (or M/Vl_w ratio) are the main factors affecting μ. For instance, for walls with $h_w/l_w = 2.0$ it would be feasible to define displacement ductility capacity values higher than those for walls with hw/lw = 0.5 or 1.0. However, for code purposes, it is unwise to provide μ values that depend on h_w/l_w or M/Vl_w ratios. This statement is based on the fact that, at the same story, all walls are subjected to practically the same value of story drift demand. Concerning the type of concrete used, significant differences among walls made of normalweight, lightweight and self-consolidating concrete were not observed. Therefore, for code-based seismic design, measured data of ductility displacement capacity were compiled in two groups according to the type of web shear reinforcement: deformed bars and welded-wire mesh (Table 3).

As expected, shear failures originating from diagonal tension or compression failure as a consequence or reversed cyclic loading involve limited ductility capacity, mainly for walls with web shear reinforcement made of welded-wire mesh. In most of these walls, the inelastic branch of the hysteresis curve was almost nonexistent because of the limited elongation capacity of the cold-drawn reinforcement used (see Table 2) and thus, displacement capacity was nearly equal to that at peak shear strength. It suggests designing such walls so that strains in reinforcement stay well below the plasticity threshold (Carrillo and Alcocer, 2012a). In contrast, in concrete walls with web shear reinforcement made of deformed bars, hysteresis curves evidenced a more ductile response. However, dramatic degradation in both stiffness and strength is the main reason of low ductility ratios; for instance, strength degradation began as soon as the peak shear was reached (Carrillo and Alcocer, 2012b).

To better understand the measured data of displacement ductility capacity μ, a statistical analysis on ductility ratios was performed; mean, standard deviation, coefficient of variation (CV), and extreme values were calculated. To aid visualizing of the statistical analysis, modified box and whisker charts were used (Fig. 6). The mean value (solid circle), standard deviation (the total height of the square represents two times the standard deviation) and extreme values (short horizontal line) are shown.

The mean value of the displacement ductility capacity (μ) of walls with web shear reinforcement made of deformed bars and welded-wire mesh is 2.88 and 2.12, respectively (Table 3). As expected, the deviation of results is high because the sample, associated to each type of web reinforcement, includes walls with different values of the h_w/l_w ratio as can be found in a house. Considering that a unique value of ductility capacity is used for designing of the entire house, a value of maximum displacement ductility capacity of 2.5 and 1.5 is proposed for code-based seismic design of low-rise housing with concrete walls whose web shear reinforcement is made of deformed bars and welded-wire mesh, respectively. These values are also shown in Fig. 6.

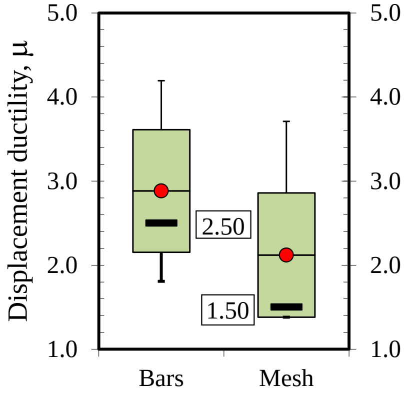

Figure 6: Statistical analysis of measured values of μ.

The value recommended for walls with deformed bars ($\mu = 2.5$) corresponds to the 42th percentile of the measured values of displacement ductility, that is, 58% of data are lower than the recommended value. In contrast, the value recommend for walls with welded-wire mesh ($\mu = 1.5$) corresponds to 7th percentile and therefore, 93% of data are lower than the recommended value. The percentages of data lower than the recommend values (58% and 93%) reflect indirectly the intrinsic safety factor related to the behavior observed in walls reinforced with the two types of web shear reinforcement. For instance, the safety factor is higher for walls with welded-wire mesh where the inelastic branch of the hysteresis curve was almost nonexistent because of the limited elongation capacity of the cold-drawn reinforcement used.

6 CONCLUSIONS

Recommendations proposed herein are based on test results obtained from an extensive experimental program that comprised 39 concrete wall specimens tested under quasi-static reversed-cyclic lateral loads and shaking table excitations. From the analysis of results, the following conclusions can be drawn:

The available ductility of structural elements and systems controlled by shear deformations should be assessed using realistic experimental techniques, as shake table and quasi-static cyclic testing.

The maximum drift ratio for evaluating ductility capacity is associated with one of the two following scenarios: when a 20% drop in peak shear strength is observed or when web shear reinforcement is fractured. In the specimens studied the first scenario occurred in walls reinforced with deformed bars; the second scenario was observed in solid walls (no openings) with web shear reinforcement made of welded-wire mesh. In case of yield displacement, it is not clearly well-defined in reinforced concrete walls controlled by shear deformations and thus, yield drift ratio is associated to the development of 80% of the maximum strength and thus, yield deformation includes the effects of cracking.

Measured data revealed that displacement ductility ratios varying between 1.63 and 2.92 may be achieved for walls with web shear reinforcement made of deformed bars, and between 1.39 and 2.71 for walls with welded-wire mesh. For code-based seismic design, a maximum displacement ductility capacity of 2.5 and 1.5 is recommended for code-based seismic design of low-rise housing with concrete walls whose web shear reinforcement is made of deformed bars and welded-wire mesh, respectively. Safety factors of recommended values were obtained from s statistical analysis of measured data and were established based on measured performance and failure modes.

Displacement ductility capacities proposed in this study can be used for estimating rationally strength modification and displacement amplification factors, because proposed ductility values are based on measured data during shake table and quasi-static reversed- cyclic testing of RC walls for low-rise housing.

Acknowledgments

The first author expresses his gratitude to the Universidad Militar Nueva Granada (UMNG, Colombia) for granting academic and research scholarships at UNAM. The authors gratefully acknowledge the financial support from Research Office (Vicerrectoría de Investigaciones) of UMNG.

References

ACI Committee 318 (2011). Building code requirements for structural concrete and commentary (ACI 318-11). American Concrete Institute, Farmington Hills, MI.

Carrillo, J., Alcocer, S. (2012a). Seismic performance of concrete walls for housing subjected to shaking table excitations. Journal of Engineering Structures 41:98-107.

Carrillo, J., Alcocer, S. (2012b). Acceptance limits for performance-based seismic design of RC walls for low-rise housing. Journal of Earthquake Engineering and Structural Dynamics 41(15):2273-2288.

FEMA-451 (2006). Recommended provisions: Design examples. Federal Emergency Management Agency, FEMA, Washington, USA.

Hsu, T., Mansour, M. (2005). Stiffness, ductility and energy dissipation capacity of RC elements under cyclic loading. Journal of Earthquake Spectra 21(4):1093-1112.

Miranda, E., Bertero, V. (1994). Evaluation of strength reduction factors for earthquake-resistant design. Journal of Earthquake Spectra 10(2):357-379.

Moroni, M., Astroza, M., Gómez, J., Guzmán, R. (1996). Establishing R and Cd factors for confined masonry buildings. Journal of Structural Engineering – ASCE 122(10):1208-1215.

Park, R. (1988). Ductility evaluation from laboratory and analytical testing. Proceedings of 9th World Conference on Earthquake Engineering – 9WCEE, Tokyo, Japan, 8:605-616.

Priestley, M. (2000). Performance based seismic design. Proceedings of 12th World Conference on Earthquake Engineering – 12WCEE, Auckland, New Zealand, paper 2831.

Salonikios, T., Kappos, A., Tegos, I., Penelis, G. (2000). Cyclic load behavior of low-slenderness reinforced concrete walls: failure modes, strength and deformation analysis, and design implications. ACI Structural Journal 97(1):132-142.

Salse, E., Fintel, M. (1973). Strength, stiffness and ductility properties of slender shear walls. Proceedings of 5th World Conference on Earthquake Engineering – 9WCEE, Rome, Italy, 918-928.

Sánchez, A. (2010). Seismic behavior of housing with concrete walls. Technical Report, Institute of Engineering, National University of Mexico, UNAM (in Spanish).

Uang, Ch. (1989). Establishing R (or Rw) and Cd factors for building seismic provisions. Journal of Structural Engineering – ASCE 117(1):19-28.